

# Dipole-Dipole interactions in Magnetocarcinotherapy (MCT)

**Marwan Rihaoui**

Physics, Winona State University, Winona, MN

LASS, T4 Atomic and Optical Physics

**Mentor name: J. Carl Kumaradas**

LANL, P-21 Biological and Quantum Physics

## Abstract

*Several new techniques for the treatment of cancer are being developed. One of these is Magnetocarcinotherapy (MCT) which is being developed in the Biological and Quantum Physics group (P-21) at LANL. MCT combines the detection, imaging, and treatment of cancer by using magnetic nanoparticles bound to monoclonal antibodies. The particles are administered to the patient through the blood stream where they bind to tumor cells. Tumors can then be detected and imaged using Superconducting Quantum Interference Devices (SQUIDs) or Magnetic Resonance Imaging (MRI).*

*The particles which are magnetic dipoles can be made to rotate by applying an external rotating magnetic field. The frictional force of the particles with the surrounding medium will cause a temperature rise that can kill tumor cells (by coagulation).*

*My research studies the effect of the dipole-dipole interactions on the heating efficiency in MCT. This can be done by comparing the strength of the magnetic field produced by rotating particles with the external rotating magnetic field. A computer model has been developed to simulate the magnetic field and heat deposition properties of particles using the finite difference method. The heating efficiency versus the particles spacing and the heating efficiency versus the external magnetic field as well as the motion of the particles will be presented.*

## Introduction

Although different types of cancer treatment had been developed, cancer treatment is still unsatisfactory. Some types of cancer treatment are: Radiotherapy, chemotherapy, and thermal therapy.

Radiotherapy is the use of high-energy radiation from x-rays, gamma rays, neutrons, and other sources. Radiotherapy uses is to kill cancer cells and shrink tumors. Radiation may come from a machine outside the body (external-beam radiation therapy), or it may come from radioactive material placed in the body near cancer cells. The radiation dose is limited by the dose to normal tissue (such as the skin).

Chemotherapy is the treatment with anticancer drugs, not limited to tumors; therefore it has dose limiting toxicity to critical organs (e.g. liver). Harm to healthy cells and that is what causes side effects.

Thermal therapy is the use of heat, is being investigated as an alternative method. The concept is that the body tissue is exposed to temperatures of 60°C-80°C for 5-10 min which damages and kills cancer cells. This technique typically uses ultrasound, microwaves, and lasers to deliver heat for the tissues. These methods have difficulty

with heating deep (e.g. CO<sub>2</sub> laser can remove thin layers from the skin's surface without penetrating the deeper layers) or large tumors and cannot be easily conformed to irregularly shaped tumors. Magnetocarcinotherapy (MCT) is a new heating method being developed at LANL that addresses these problems. It uses modified magnetic nanoparticles which bind specifically to tumor tissue. The tumor is then heated by spinning the particles using a rotational external magnetic field  $B_{ext}$ .

Current MCT models do not account for the interaction between particles. This paper investigates the effect of these interactions on the heating efficiency and the motion of the particles during MCT.

### MCT Concept

Nanomagnetic particles are attached to monoclonal antibodies that enable them to bind to the tumor's receptor. The geometry of the antibody should match the receptor of the tumor. Once a tumor has been detected, nanoparticles (SmCo<sub>5</sub>) which are coated with gold (Au, does not react with anything in the body), attached to monoclonal antibodies, and then injected to the blood stream, Figure 1.

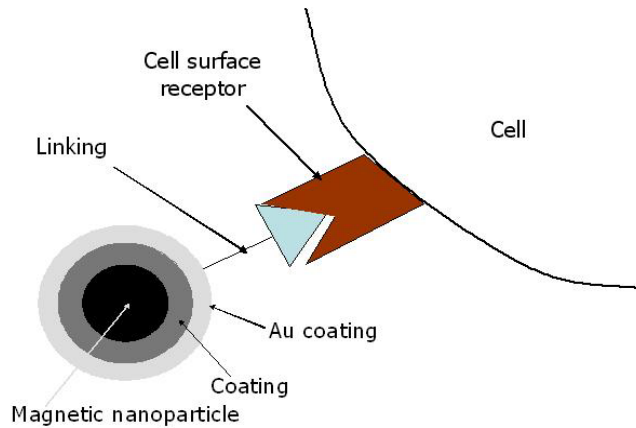


Figure1. Magnetic nanoparticles (SmCo<sub>5</sub>) coated by gold are attached to a monoclonal antibody that will bind to the tumor's receptor.

We expect to need a magnetic field that is 100-300G, rotating in the 1-5 MHz range. Figure 2 shows the magnetic coil concept for generating a rotational magnetic field. A sinusoidal wave signal is applied across the coils with different phase difference (45°, 90°, and 135°). For example, two pairs of coils that are 0 and 90 degrees out of phase will generate a rotational magnetic field. The other two pairs of coils, the 45 and the 135 degrees, insure a smooth circular rotation for the generated magnetic field.

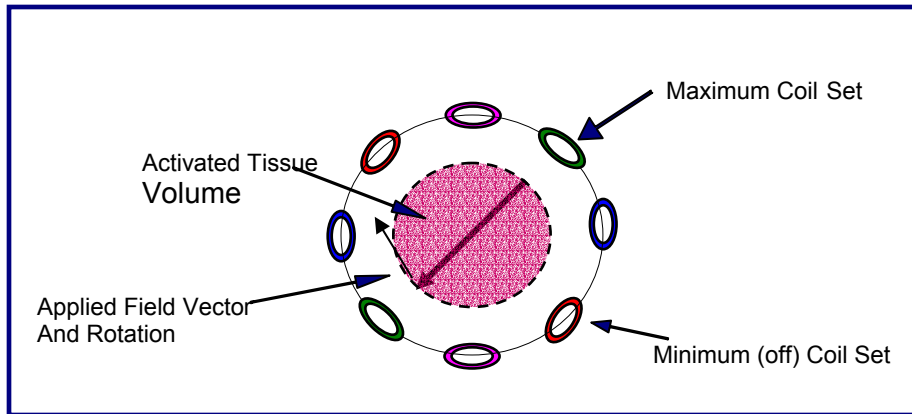


Figure2. The pink and the blue pair of coils are those that are 0 and 90 degrees out of phase, the green and the red pair of coils are the 45 and 135 degrees out of phase. The figure shows the  $B$  field direction (in the middle) when the green coil (135 degree out of phase with the bottom pink coil) is at the maximum peak and the red coil (45 degrees out of phase with the bottom pink coil) is at a minimum peak.

In addition to treating the tumors, MCT particles has the ability to detect small tumors that are not detectable by current imaging techniques. The detection of the tumor is done using Los Alamos MEG system, Figure 3.



Figure3. The MEG system at LANL for detecting tumor cells by measuring the magnetic field from the head.

The MEG system measures the magnetic field  $B$  at the surface of the head using SQUIDs. From that field we can trace the current producing this field. The imaging component of the MCT system uses the same principle where the  $B$  field is produced by the magnetic particles in the tumor.

The external magnetic field  $B_{\text{ext}}$  will cause the nanomagnetic particles to rotate in their medium (the tumor). The rotation will yield a friction between the particles and the tumor and heat will be generated. The heat generated from the friction will destroy the tumor by coagulating the proteins in the tissue. Studies had been done to determine the characteristics of the particles needed and their distribution:

- Particle radius needs to be less than 100nm.
- Expect  $10^5$  to  $10^6$  particles/mm<sup>3</sup> and from that the particles separation would be 0.5 to 5  $\mu$ m.

### Viscous Heating by Rotating Particles

Viscosity opposes the rotation of the particles by magnetic field. At a value for the magnetic field  $B_{crit}$  such that:

$$B_{crit} = \frac{6\eta\omega}{M} \quad (1)$$

the magnetic torque balances the viscous torque, resulting in maximal heating rate  $P_{high}$  given by:

$$P_{high} = 8\pi\eta\omega^3 a^3 \quad (2)$$

If  $B$  is less than  $B_{crit}$ , current model (done by Dr. B Wright in P-21 at LANL) indicates that the heating rate  $P_{low}$  is:

$$P_{low} = \left(\frac{B}{B_{crit}}\right)^2 P_{high} = \frac{2\pi B^2 \omega^2 M^2 a^3}{9\eta} \quad (3)$$

where  $\eta$  is the viscosity of the medium,  $\omega$  is the angular velocity of the applied magnetic field, and  $M$  is the magnetization of the particle. Equation (3) assumes that there is no dipole-dipole interaction between the particles. The goal of this project was to determine how the dipole-dipole interactions between the particles affect the heating efficiency of the system. The heating efficiency of the system defined as  $E = P_{sim}/P_{low}$  where  $P_{sim}$  is the average heating rate of the particles.

Figure 4 shows the temperature rise of the tumor versus the magnetic field external  $B_{ext}$ , the driven frequency of the magnetic field is 1MHz and heating time duration of 10 s. Using particles of 500nm radius and a separation of 10  $\mu$ m. From the graph we see that 100 – 200 G produces a 2°C-7°C rise in temperature in a period of 10 s, which is the hating rate desired in thermal therapy.

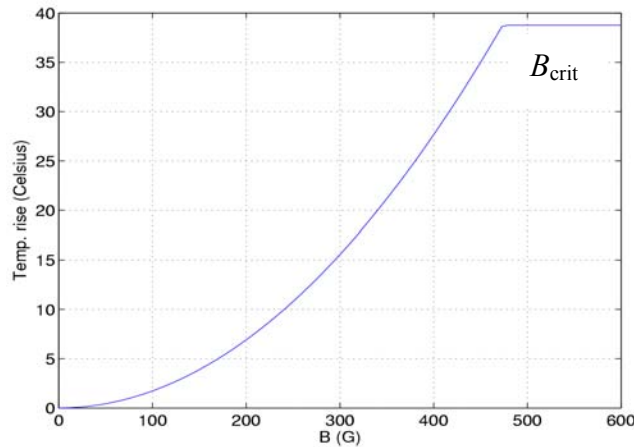


Figure4. Temperature versus the applied external magnetic field  $B_{ext}$ ,  $B_{crit}$  is the value where the curve level off.

## The Model and the Equation of Motion

Figure 5 provides a schematic diagram of the model used for the particle-particle interactions. It consists of a sphere of water with  $N$  randomly distributed particles with an average separation  $s$  with the constraint that  $s > 2a$ . Other parameters used in the model are:

- The magnetization of a particle,  $M = 800,000 J/Tm^3$ .
- The radius of the particle,  $a = 50nm$ .
- The viscosity of water,  $\eta = 10^{-3} Ns/m^3$ .
- The frequency of the applied circular external magnetic field,  $f = 3.8MHz$ .

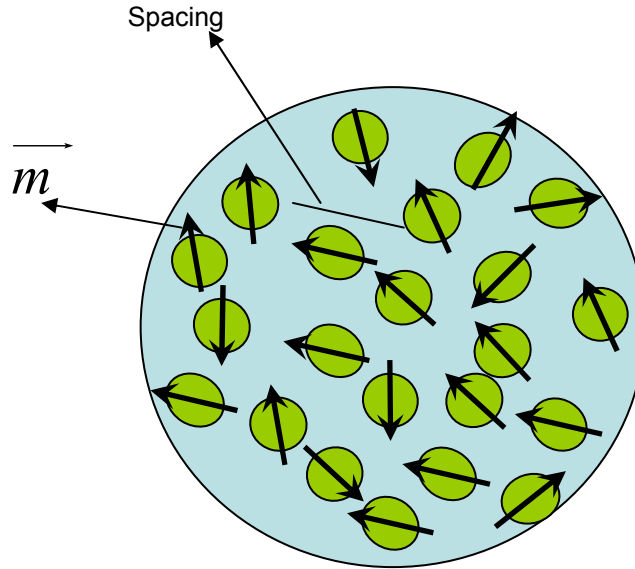


Figure5. The model we are trying to solve,  $N$  magnetic particle with magnetic dipole  $m$  flowing in a viscous medium (water).

### The motion of the particles:

Let the direction of particle  $k$  defined by  $e_k$  such that:

$$\hat{e}_k = \frac{\overrightarrow{m}_k}{|\overrightarrow{m}_k|} \quad (4)$$

Where  $m_k$  is the dipole moment of particle  $k$ . If we neglect the rotation of the particle around the axis  $e$  and at low inertia limit, the torque  $T_k$  acting on the particle is zero:

$$\overrightarrow{T}_k \times \hat{e}_k = 0 \quad (5)$$

The torque consists of two components; the torque due to the magnetic field,  $T_M$ , and the torque due to the viscous drag,  $T_V$ :

$$\begin{aligned}\vec{T}_k &= \vec{T}_M + \vec{T}_V \\ &= |\vec{m}_k| \hat{e}_k \times \vec{B}_k + (-8\pi\eta a^3 \hat{e}_k \times \dot{\hat{e}}_k)\end{aligned}\quad (6)$$

where  $B_k$  is the total magnetic field at particle  $k$  due to the other particles. The magnetic field at point  $P$  due to a magnetic dipole  $m$  at a distance  $r$ , Figure 6, is:

$$\vec{B}_{dp}(\vec{r}) = \frac{\mu_o}{4\pi |\vec{r}|^3} (3(\vec{m} \cdot \hat{r})\hat{r} - \vec{m}) \quad (7)$$

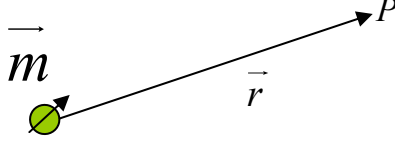


Figure6. A point  $P$  at a distance  $r$  from a magnetic dipole  $m$ .

At any dipole  $k$ , the magnetic field  $B_k$  is the external magnetic field  $B_{ext}$  plus the magnetic field from the other dipoles:

$$\vec{B}_k = \vec{B}_{ext} + \sum_{\substack{i=1 \\ i \neq k}}^N \vec{B}(\vec{r}_i) \quad (8)$$

Using some scaled parameter:

$$S_0 = \frac{MB_{0,k}}{6\eta\omega} \quad (9)$$

where:  $\vec{B}_k = B_{0,k} \vec{\beta}_k$ , such that

$$\langle |\vec{\beta}_k|^2 \rangle = 1$$

From equations (5), (6), and (9) combined to scaled equation of motion:

$$\frac{1}{\omega} \dot{\hat{e}} - S_0 (\vec{\beta} - (\hat{e} \cdot \vec{\beta})\hat{e}) = 0 \quad (10)$$

Equation (8) is a first order differential equation for the motion of a particle. The heating efficiency  $E$  is directly proportional to the rate of change of the direction of the particle. If we define  $u$  such that:

$$u_k = \frac{1}{\omega} \dot{\hat{e}} = S_0 (\vec{\beta}_k - (\hat{e} \cdot \vec{\beta}_k)\hat{e}) \quad (11)$$

Then the heating efficiency  $E$  is:

$$E = \frac{1}{N} \sum_{k=1}^N a_k^3 \langle |u_k|^2 \rangle \quad (12)$$

The code was initially written in MatLab to solve equation (10) using Euler’s method. Subsequently, the “ode45” routine in MatLab was used in attempt to speed up the run time of the simulations. The “ode45” routine was a Runge-Kutta method and implements a variable adoptive time step. Its use resulted in more than a twenty fold reduction in the run time. A simulation with 100 particles required three hours on a Pentium Xeon 2.8GHz system to simulate 6000 cycles of particle rotations.

## Results

Figure 7 shows a plot for the heating efficiency versus  $s/a$ , where  $s$  is the average spacing between the particles and  $a$  is the radius of a particle. Notice that  $E$  is maximum for  $s/a = 30$ . The heating efficiency  $E$  drops with decreasing  $s/a$  below 30, the particles are coupled together which implies less spacing to move freely to generate heat. The heating efficiency  $E$  also drops with increasing  $s/a$  above 30, the particles are far away from each others which implies less interactions. It is puzzling why the heating efficiency is maximum at  $s/a = 30$ . We will look into this effect in more details later in this section.

Figure 8 shows the heating efficiency of the external magnetic field  $B_{ext}$ . The blue in the graph includes coupling (dipole-dipole interactions), and the green does not include dipole-dipole interactions. If we look at the percentage of the heating efficiency with coupling effects as a percentage of no coupling effects, this percentage increases with increasing  $B_{ext}$ .

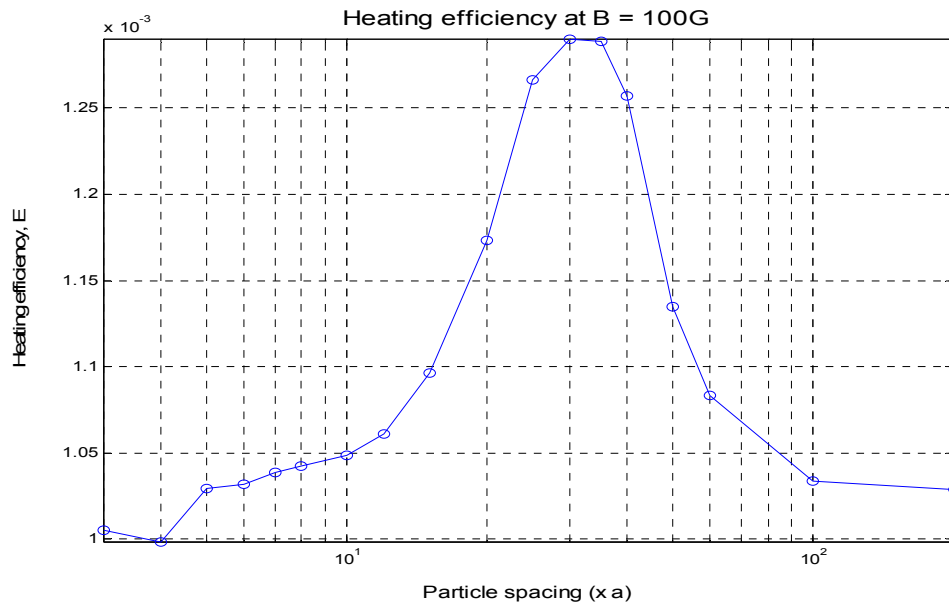


Figure7. The graph for the efficiency versus the particle spacing, the particles spacing range is the same one predicted for the treatment ( $s/a = 10$  to  $100$ ).

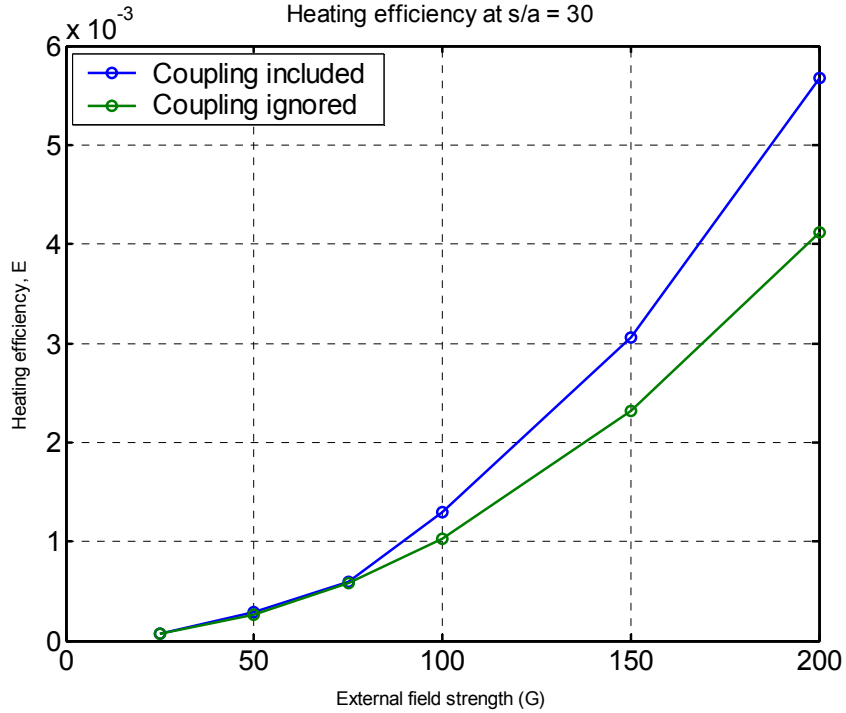


Figure8. The plot for the efficiency versus the external magnetic field  $B_{ext}$ , the blue curve is the case where the dipole-dipole interactions is included, the green curve is the case with no interactions.

To understand what is happening for the particles at the maximum  $s/a = 30$  we chose two values of separation to compare. Case 1 for  $s/a = 5$  where the efficiency is low, and case 2 for  $s/a = 30$  where the efficiency is maximum. We studied the two cases for four random particles as a function of two angles,  $\theta$  and  $\phi$  (refer to figure 9), and the results are presented in figures 10 – 13:

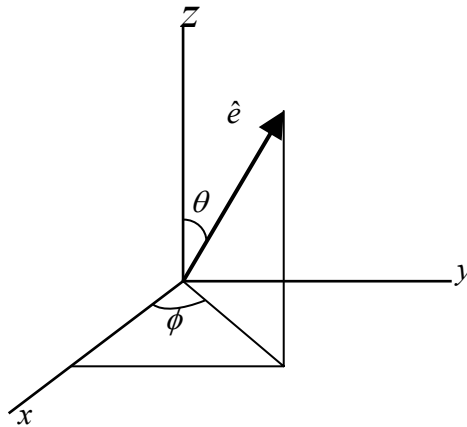


Figure9. In the spherical coordinates  $\theta$  is the angle from the z-axis (goes from 0 to  $\pi$ ) and  $\phi$  is the angle in the xy-plane (goes from 0 to  $2\pi$ ).

Case 1 for  $s/a = 5$ : The efficiency drops down to a constant value and remains at a steady state (Figure 10). To understand this effect, Figure 11 shows the motion of four random particles. For example, after 20 revolutions the blue particle oscillates around a

fixed angle  $\phi = 155^\circ$  (from the z-axis). In the xy-plane, it decreases from  $180^\circ$  to  $100^\circ$  after 20 revolutions, and then keep oscillates at  $100^\circ$ . When these components of motion are combined, the motion of the particle in three dimensions is similar to a top spin that is précinging around a fixed axis.

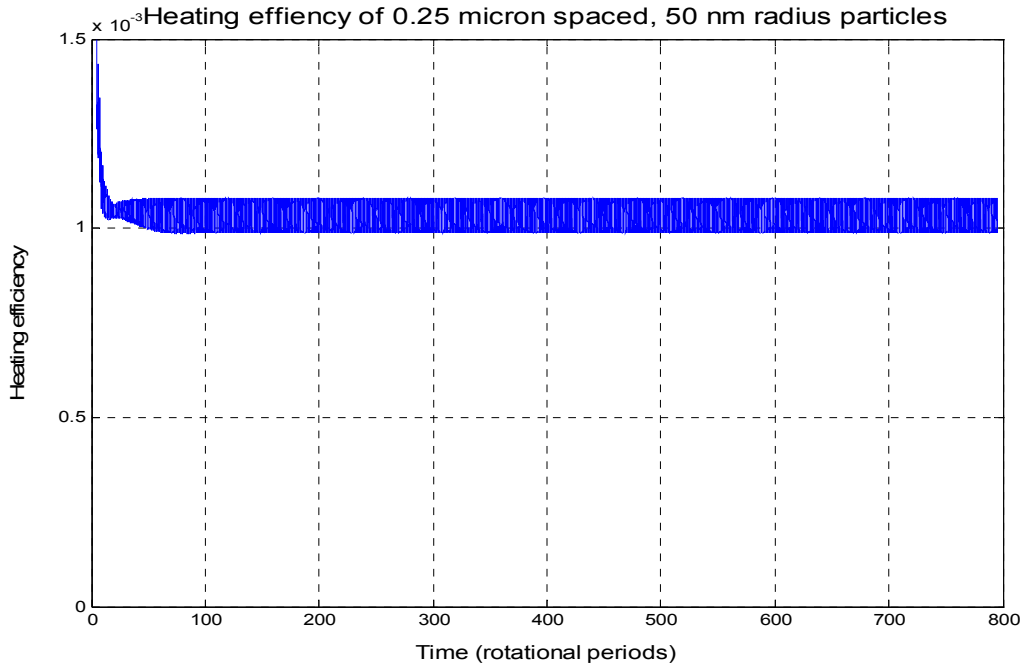


Figure10. The heating efficiency for  $s/a = 5$  versus time.

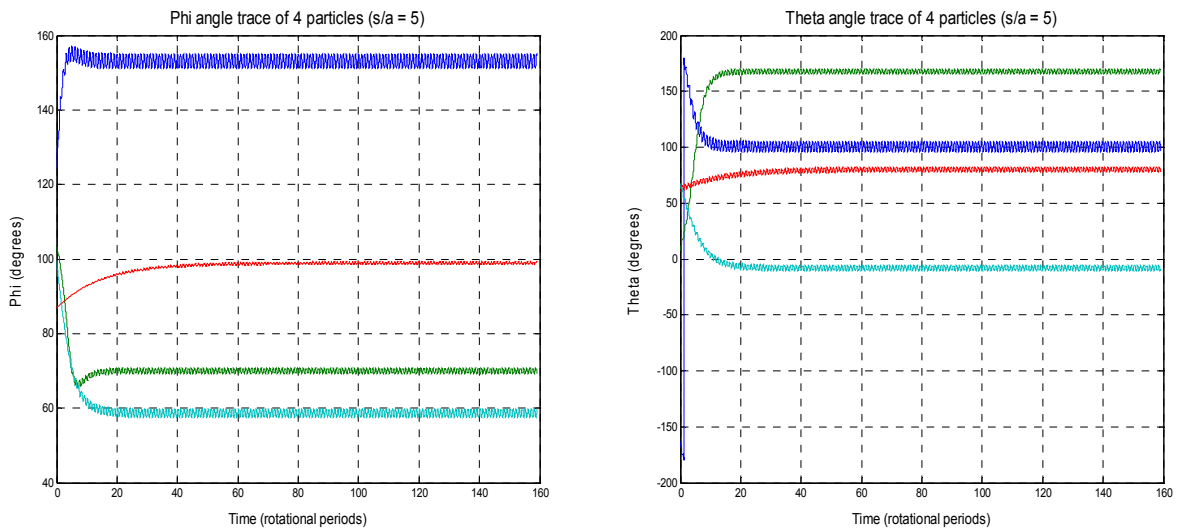


Figure11. To the left is the graph for the  $\phi$  angle and for the right is the graph for the  $\theta$  angle, case of  $s/a = 5$ .

Case 2 for  $s/a = 30$ : Compared to the  $s/a = 5$  case the efficiency takes more time to reach a steady state (Figure 12). In the  $\phi$  direction the red particle is oscillating and going down the xy-plane. But in the xy-plane it's oscillating back and forth. This motion yield a precession rotation around a second axis and the particle is moving along with that. This highly non-linear motion may explain why there is a higher heating efficiency at  $s/a = 30$ , this needs to be studied more in details.

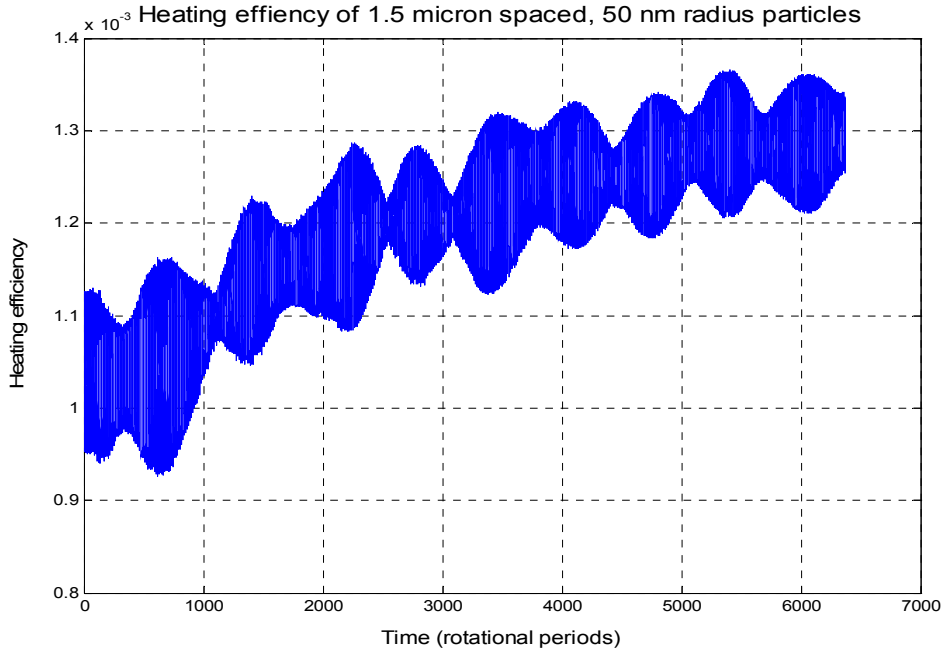


Figure12. The heating efficiency for  $s/a = 30$  versus time. The efficiency varies significantly.

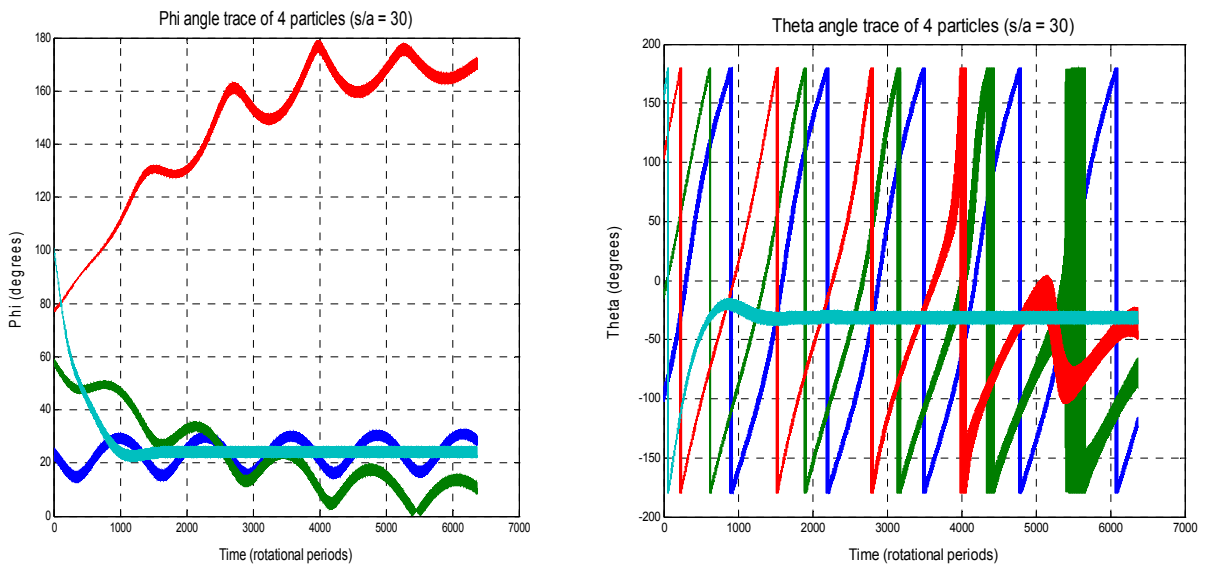


Figure13. To the left is the graph for the  $\phi$  angle and for the right is the graph for the  $\theta$  angle, case of  $s/a = 30$ .

## **Conclusion**

The results from the simulations were unexpected. The most unexpected behavior was the motion of the particles at an average spacing  $s = 30a$ . The first thing to notice is that at maximum efficiency (spacing equal to  $30a$ ), the coupling effect increases the heating efficiency by 30%. Secondly the increase in heating efficiency with coupling effects as a percentage of the heating efficiency with no coupling effects increases with increasing  $B_{\text{ext}}$ .

## **Acknowledgement**

I would like to thank the LASS for choosing me in this program. I would like to thank the people responsible for the success of this program: Beverly James, Lee Collins, Daniel James, Stephane Mazevet, Sally Seidel, and Norm Magee. Also I would like to thank all the people at P-21 division and a special thank for my mentor Dr J. Carl Kumaradas for his helping, his mentoring, and his patience.